Electronic Supplementary Information

Exploring fuel cell cathode materials using ab initio high throughput calculations and validation using carbon supported Pt alloy catalysts.

M. Sarwar[a], J.L. Gavartin[b†], A. Martinez Bonastre[a], S. Garcia Lopez[a], D. Thompsett[a], S. Ball[a] A Krzystala[b], G. Goldbeck[b‡] and S.A. French[a]

a) Johnson Matthey Technology Centre, Blounts Court, Sonning Common, Reading, RG4, 7QE, United Kingdom

b) Accelrys (now BIOVIA) Ltd, 334 Cambridge Science Park, Cambridge, CB4 0WN, United Kingdom

†now at Schrodinger, 20 Station Road, Cambridge, CB1 2JD

‡now at Goldbeck Consulting, St John's Innovation Centre, Cowley Road, Cambridge CB4 0WS, UK

1. 1 Calculation Methods

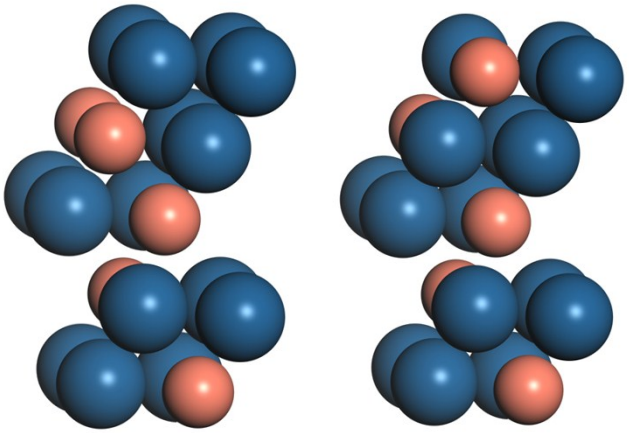

Pt_3M skin Pt_3M seg

Figure S1: 2x2 supercell cell adopted for Pt_3M alloys. The model on the left consists of a Pt skin and enrichment of M subsurface. This is referred to as the Pt_3M skin model. The model on the right has a Pt_3M composition in each layer and is referred to as the Pt_3M seg model.

	a, b (Å)	c (Å)	E_{ads} O (eV)	E_{ads} OH (eV)
Ni	**3.57**	**-**	**-4.72**	**-3.39**
Co	**2.54**	**4.11**	**-4.88**	**-5.93**
Pd	**3.95**	**-**	**-3.97**	**-2.68**
Rh	**3.90**	**-**	**-5.35**	**-3.20**
Ru	**2.73**	**4.30**	**-5.44**	**-3.50**
Os	**2.76**	**4.35**	**-5.24**	**-3.30**
Ir	**3.91**		**-4.07**	**-2.92**
Cu	**3.68**		**-4.10**	**-3.23**
Pt	**4.01**		**-3.40**	**-2.68**
Ag	**4.19**		**-2.81**	**-2.68**
Au	**4.23**		**-2.20**	**-1.85**
Nb	**3.33**		**-7.23**	**-5.13**
Cr	**2.87**		**-7.02**	**-4.77**
Ta	**3.37**		**-6.82**	**-4.92**
Hf	**3.24**	**5.14**	**-7.40**	**-5.63**
V	**3.02**		**-7.44**	**-5.38**
Y	**3.7**	**5.82**	**-7.75**	**-5.62**
Fe	**2.85**		**-5.85**	**-4.23**
Ti	**2.98**	**4.68**	**-8.36**	**-5.70**
Zr	**3.26**	**5.20**	**-8.35**	**-5.68**
Sc	**3.36**	**5.24**	**-8.89**	**-6.03**

Table S1: Lattice parameters, adsorption energies and binding sites for monometallic surfaces.

	Lattice Parameter (Å)	E_{ads} (eV) O on Pt_3M skin model	E_{ads} (eV) OH on Pt_3M skin model	E_{ads} (eV) O on Pt_3M seg model	E_{ads} (eV) OH on Pt_3M seg model
Pt_3Ni	**3.93**	**-3.07**	**-2.46**	**-3.82**	**-2.66**
Pt_3Co	**3.94**	**-3.17**	**-4.77**	**-4.09**	**-5.56**
Pt_3Pd	**4.00**	**-3.40**	**-2.44**	**-3.50**	**-2.60**
Pt_3Rh	**4.01**	**-3.13**	**-4.52**	**-3.39**	**-4.86**
Pt_3Ru	**3.97**	**-3.22**	**-2.46**	**-4.19**	**-3.22**
Pt_3Os	**3.97**	**-3.18**	**-2.51**	**-4.79**	**-3.55**
Pt_3Ir	**3.99**	**-3.17**	**-2.43**	**-3.51**	**-2.92**
Pt_3Cu	**3.94**	**-3.06**	**-2.38**	**-3.46**	**-2.67**
Pt_3Ag	**4.04**	**-3.45**	**-2.49**	**-3.40**	**-2.69**
Pt_3Au	**4.06**	**-3.60**	**-2.59**	**-3.37**	**-2.57**
Pt_3Fe	**3.95**	**-3.18**	**-2.46**	**-8.85**	**-3.31**
Pt_3Nb	**4.03**	**-2.89**	**-2.35**	**-6.51**	**-4.68**
Pt_3Cr	**3.96**	**-3.23**	**-2.61**	**-5.68**	**-3.87**
Pt_3Ta	**4.06**	**-3.16**	**-2.39**	**-5.37**	**-4.44**
Pt_3Hf	**4.09**	**-3.17**	**-2.43**	**-4.39**	**-3.87**
Pt_3V	**3.96**	**-2.92**	**-2.28**	**-6.27**	**-4.19**
Pt_3Y	**4.22**	**-3.67**	**-2.61**	**-4.33**	**-3.58**
Pt_3Ti	**3.98**	**-2.98**	**-2.38**	**-4.98**	**-4.16**
Pt_3Zr	**4.07**	**-3.08**	**-3.18**	**-5.48**	**-5.06**
Pt_3Sc	**4.04**	**-3.21**	**-2.41**	**-4.89**	**-4.23**

Table S2: Adsorption energies for Pt_3M alloys

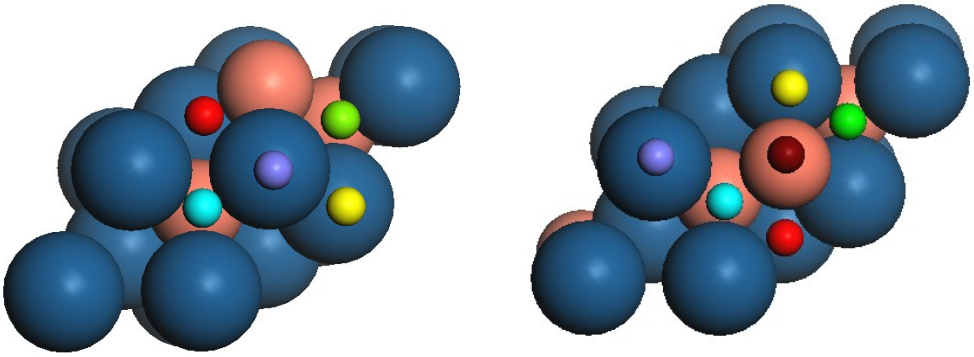

Figure S3: adsorption sites modeled on Pt_3M–skin (left) and Pt_3M segregated (right) structures. Red spheres indicate fcc site 1 (Pt), green fcc site 2 (M), yellow hcp site 1 (Pt), blue hcp site 2 (M), purple top 1 (Pt) and brown top2 (M)

1.2 Experimental Details

1.3.1 Catalyst Preparation

Pt and Pt alloy catalysts were prepared using a previously reported general method[1,2]. In brief, Pt and the base metal were precipitated onto a high surface area carbon black in an aqueous slurry using base hydrolysis. On completion of metal deposition, the slurry was filtered and washed to remove salts. The filter cake was then dried and then annealed to temperatures between 900 and 1200°C in either an Ar or H_2 atmosphere to induce reduction, alloying and modest sintering.

1.3.2 Catalyst Characterisation

Catalysts were characterized for total metal content (inductively coupled plasma emission spectroscopy (ICP-ES), active metal area (gas-phase CO chemisorption), average Pt crystallite size (X-ray Diffraction, peak line broadening using Rietveld analysis) and degree of alloying (XRD, shift in Pt lattice parameter away from pure Pt (a = 3.923Å)). A summary of the characterisation data is shown in Table S3.

1.3.3 Catalyst Leaching Studies

The stability of metal, M to the acidic environment of the PEMFC was investigated using two approaches.

Simple acid leaching: Catalyst samples were stirred in 0.5 M H_2SO_4 (slurry concentration 10 g l^{-1}) at 80°C for 24 hrs and the subsequent leachates were analysed for Pt and M content using ICP-ES.

Low electrolyte volume cell leaching: This used a method previously reported method[3]. Electrodes of the catalyst samples were prepared by painting a catalyst ionomer mixture onto a gas diffusion media at a Pt loading of 0.4 mg(Pt) cm^{-2} geometric. Electrode samples (3.1 cm^2) were heat treated at 177°C for 2 min then fully wetted in water, then placed in a 3 electrode electrochemical cell containing 100 cm^3 of 1M H_2SO_4 electrolyte at 80°C. The electrodes were then voltage cycled between 0.6 and 1.2 V vs RHE using a saw-tooth wave for 1000 cycles. The electrolyte was sampled periodically and analysed using ICP-MS (ICP-mass spectroscopy) to determine leached Pt and M contents.

1.3.4 Membrane Electrode Assembly (MEA) Fabrication and Testing

MEA Fabrication: Cathode electrodes of the catalyst samples were prepared by coating a catalyst ionomer mixture onto Toray TGP60 gas diffusion media at a Pt loading of 0.2 or 0.4 mg(Pt) cm^{-2} geometric. A Pt/C electrode was used as an anode. MEAs were fabricated from 50 cm^2 electrodes, by hot-pressing the anode and cathode against Flemion SH-30 (Ashai Glass) or Nafion NRE112 CS (DuPont) membrane.

Single cell testing: MEAs were tested in 49 cm^2 hardware at 100% Relative Humidity (RH) using external contact humidifiers and at 80°C and 150 kPa absolute pressure. MEAs were conditioned using H_2/air feeds at a stoichiometry of 2:2 and for activity determination (oxygen polarization) using H_2/O_2 feeds at a stoichiometry of 2:10. Samples were conditioned in the single cell for at least 8hrs on H_2/Air. Membrane resistance was measured using the current interrupt technique and measured currents were corrected for H_2 crossover, measured in situ for each MEA. O_2 reduction activity was determined galvostatically by imposing a current (current density by dividing by electrode area) and measuring the voltage when stable. A steady state polarisation curve was determined from different i-V points and extrapolated to 900 mV to give a current to determine standard activity (see Figure S8). Mass and specific activity was derived from this current by dividing by either the Pt electrode loading (mA mg^{-1} Pt) or the in-situ Pt area (μA cm^{-2} Pt actual area).

Measurement of in-situ MEA cathode Pt area was carried out using cyclic voltammetry. CO area was measured at 80°C in the MEA by poisoning the cathode with CO at 0.15V (vs RHE), purging with N_2 at 0.15V, then cycling from 0.15 to 1V and integrating the area of the CO peak, using a correction factor of 420μC cm^{-2} Pt.

In general two MEAs were fabricated and tested for each catalyst. Therefore, quoted mass and specific activity values represent averages of each individual catalyst tested.

Pt_3M	%Pt	%M	Pt:M	XRD			CO metal area /m^2 g^{-1} Pt	Echem CO metal area /m^2g^{-1} Pt	% M leached		Mass Activity (A/mgPt)	Spec Activity (μA/cm2-Pt)
				Cryst size/nm	Lattice parameter, a/Å expt	Lattice parameter, a/Å theory			static	cycled	@ 900mV, iR free, 150kPa O_2	
Al	38.2	1.2	77:23	5.1	3.876	3.876	31	38	31	44	0.14	381
Sc	40.8	3.7	79:21	5.9	3.951	3.953	27	37	22	38	0.13	460
Ti	39.5	3.7	73:27	3.5	3.903	3.897	38	53	43	59	0.18	349
Cr	39.4	2.8	79:21	4.8	3.876	3.871	34	26	15	39	0.20	714
Fe	57.3	5.4	75:25	5.6	3.869	3.872	27	nd	25	nd	nd	nd
Co	39.5	4.0	75:25	5.9	3.848	3.854	40	34	27	18	0.26	963
Ni	43.1	4.3	75:25	*c.* 9	3.840	3.848	30	27	20	nd	0.19	704
Cu	25.0	3.6	69:31	3.2, 3.7	3.732, 3.829	3.848	108	127	nd	nd	0.13	678
Y	41.1	6.0	76:24	nd	"Pt_3Y"	4.075	2	20	nd	nd	0.07	327
Zr	43.8	5.3	79:21	8.4	3.940	3.990	31	32	27	62	nd	nd
Hf	39.4	10.2	78:22	5.7	3.970	3.981	29	32	17	45	nd	nd
Ta	38.1	11.5	75:25	nd	"Pt_4Ta, Pt_3Ta"	5.538*	13	25	5	0	0.04	500
Ir	44.6	14.7	75:25	nd	mixed	3.896	42	33	nd	nd	0.09	275
Pt	40.1		100	7.7	3.924	3.923	28	21	0	3	0.13	611

*-orthorhombic, nd – not determined

Table S3. Representative carbon supported Pt_3M alloy catalyst physical and electrochemical properties

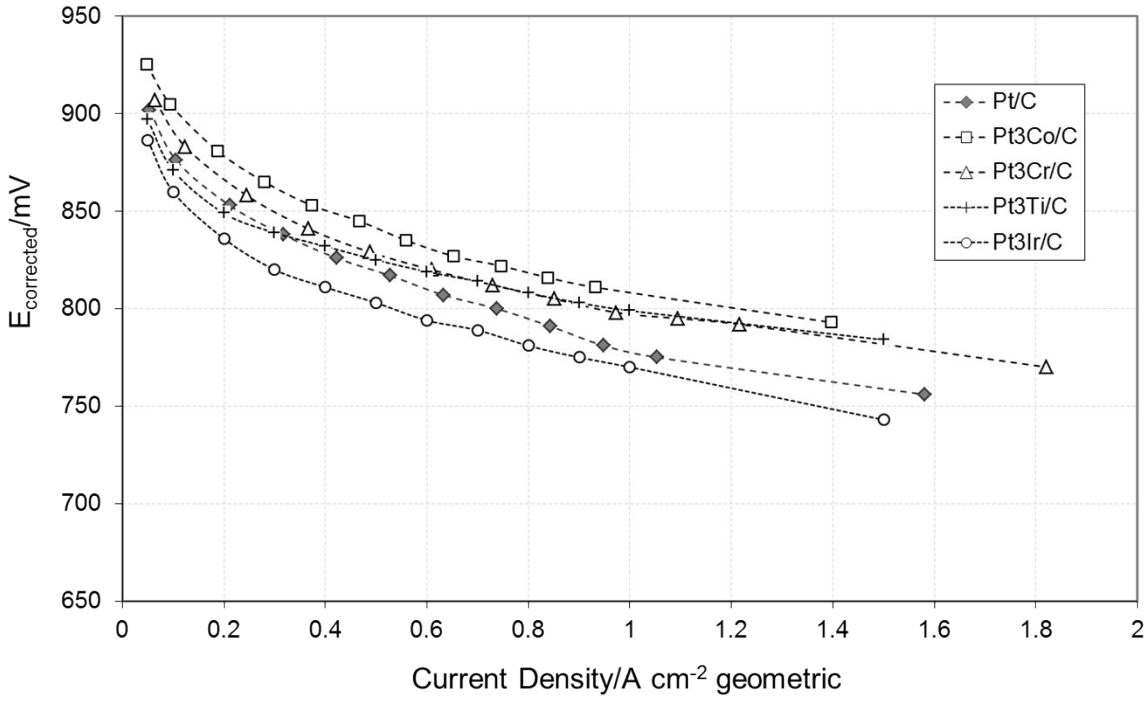

Figure S4. Representative H_2/O_2 polarisation curves for a number of catalysts

Figure S4 shows H_2/O_2 polarisation curves for a number of Pt and Pt alloy catalysts as cathode layers within MEA structures. Comparison activity points have been taken at 900 mV (corrected for internal resistance) to give the basis of the mass and specific activity values shown in Table S.

1.4. Leaching Results

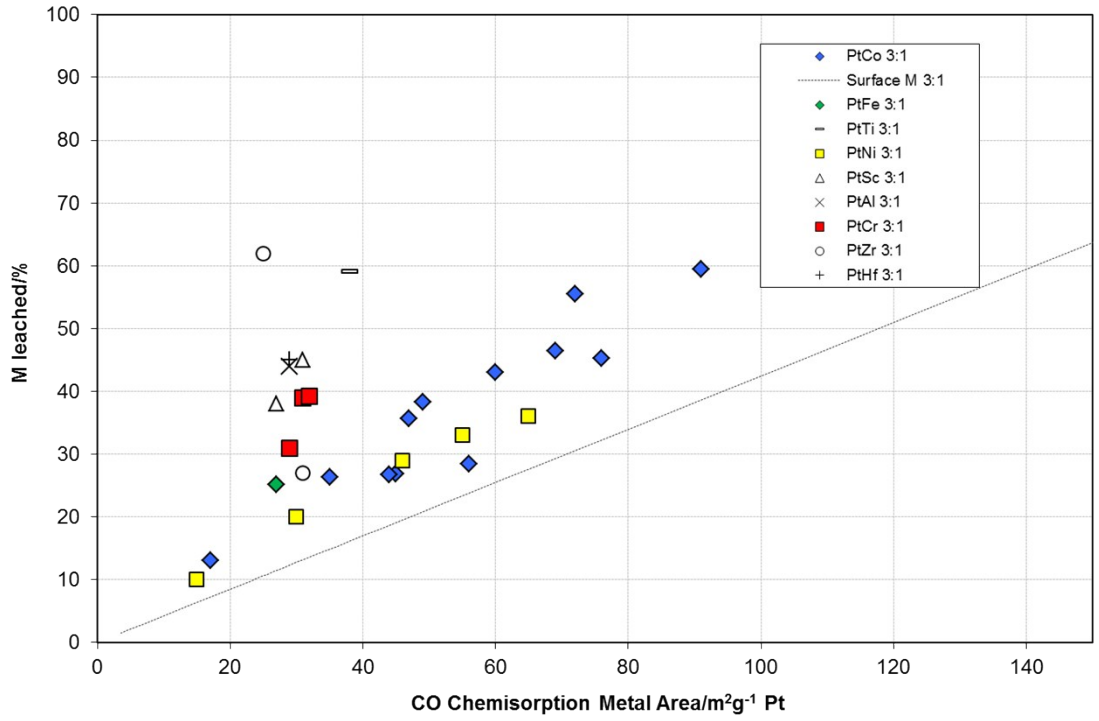

Figure S5. Amount of leached M as a function of Pt metal surface area for a range of Pt_3M catalysts (combination of static and cycled leached data).

The dotted line represents that amount of M that would leached if the surface composition was 3:1, assuming only M at the surface is removed. This is calculated using a cubo-octahedral particle model based on the numerical expression reported in Benfield[4]. The statically leached data is shown by filled symbols, while electrochemically cycled data is shown by open symbols.

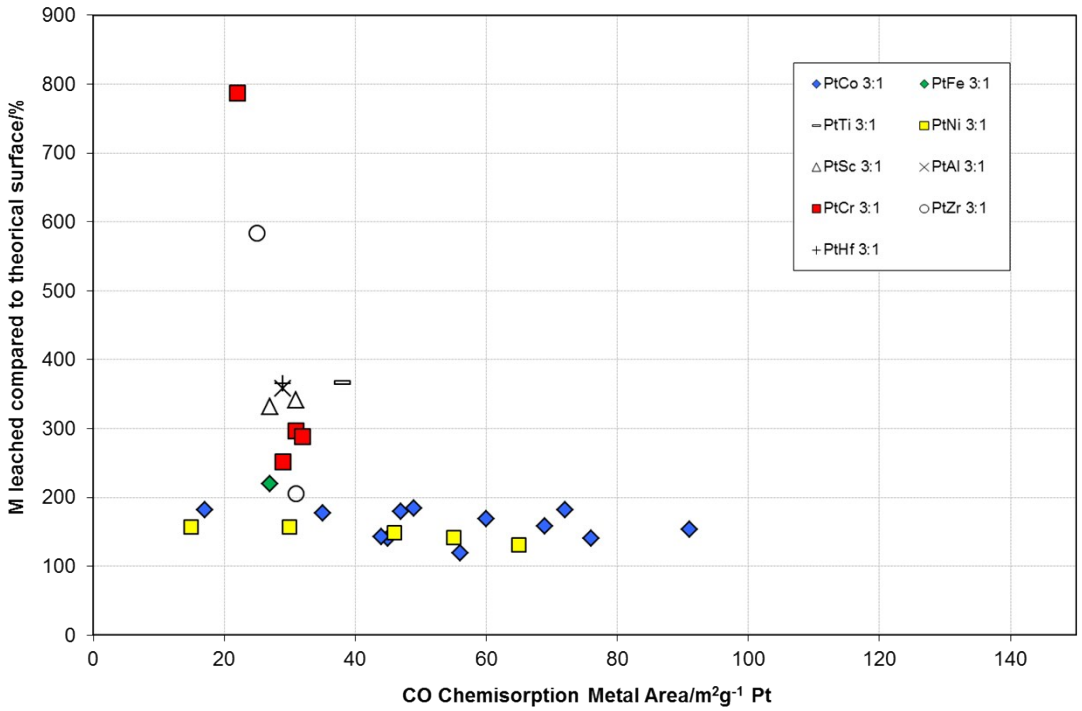

Figure S6. Amount of M leached expressed as a percentage above that expected from a perfect 3:1 surface particle model (100% represents a perfect 3:1 surface) as a function of Pt metal surface area.

The results fall into two groups. Pt alloys with M's which have low electro-positivity (M = Fe, Co, Ni) show relatively low excess metal removal (up to 2 times nominal), while Pt alloys with M's with higher electro-positivies (Sc, Ti, Zr, Hf, Cr Al) all show higher excess metal removal (up to 8 times nominal). These results are despite the fact that all these Pt alloys show Pt lattice parameters from XRD that are consistant with full alloying.

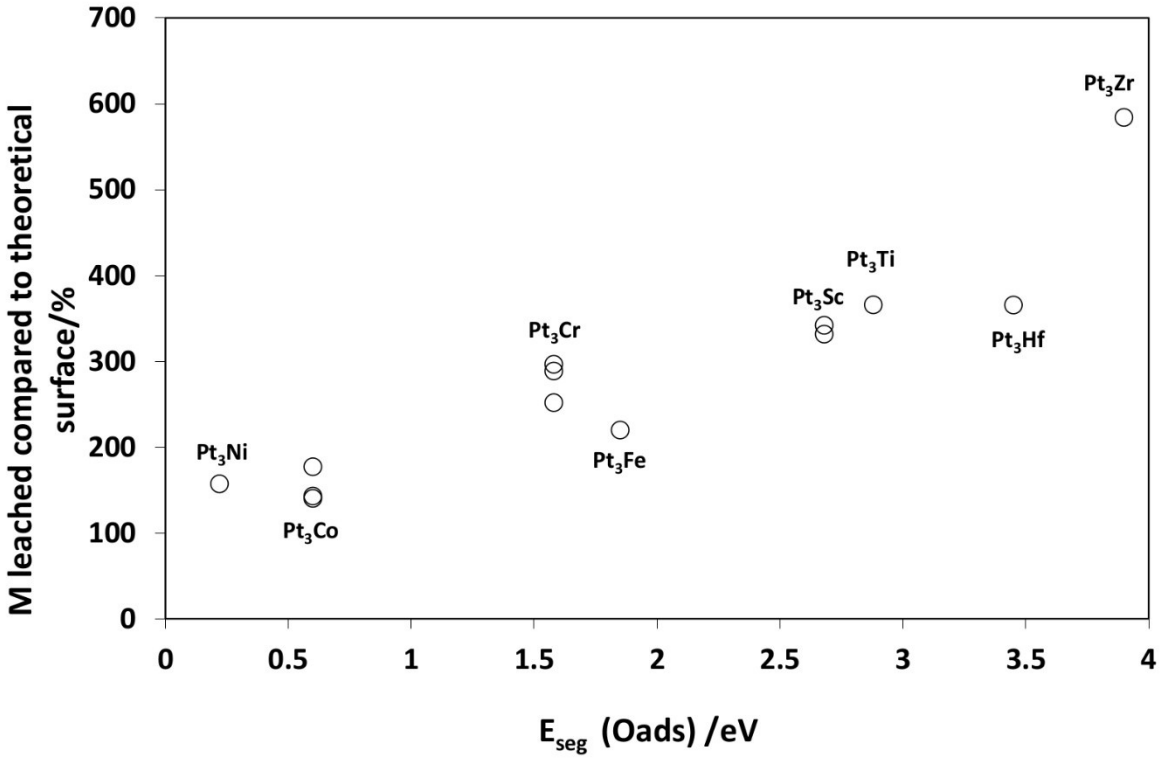

Figure 8b. M leached as a percentage above that expected for a non-segregated Pt_3M surface as a function of O induced segregation energy for Pt_3M catalysts with a Pt surface area of 30 ± 10 $m^2\ g^{-1}$ Pt.

The plot shows a reasonable correlation of increasing M leached with increasing Oads induced segregation energy. Given that it has been previously shown that acid leaching only occurs at the surface, this would indicate that the O induced segregation energy predicts surface M composition.

1.5 Activity – modelling correlations

Correlations with d band and O_{ads} of Pt skin surfaces

The O_2 reduction specific activity has been initally been correlated with the Pt skin surfaces. These surfaces have 2 O adsorption sites; one above a Pt in the sub-layer and one above a M atom in the sub-layer. The O above a sub-layer M has the higher binding energy.

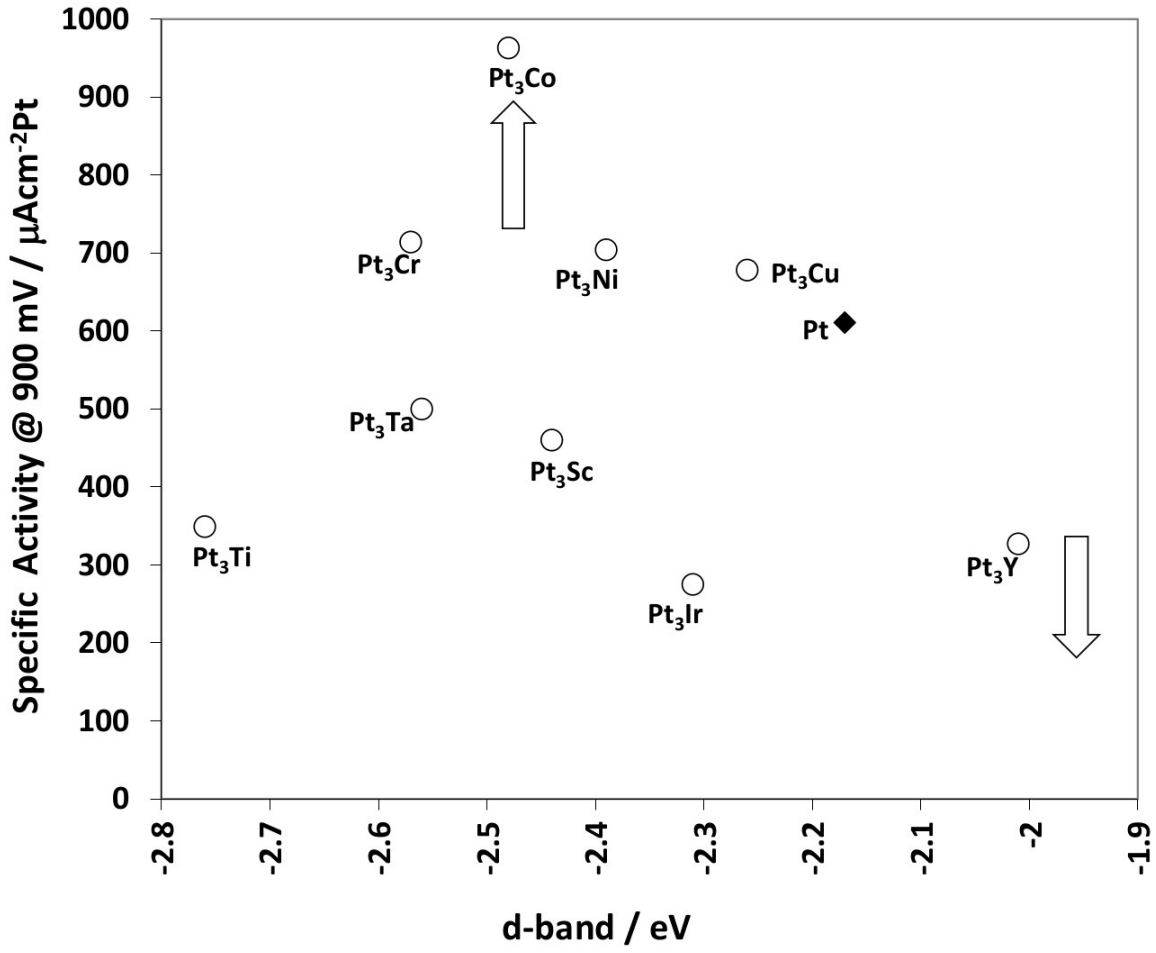

Figure 9. O_2 reduction specific activity at 900 mV as a function of surface d-band centre

There appears a relatively poor correlation of surface d-band centre energy with O_2 reduction activity for the Pt skin surfaces.

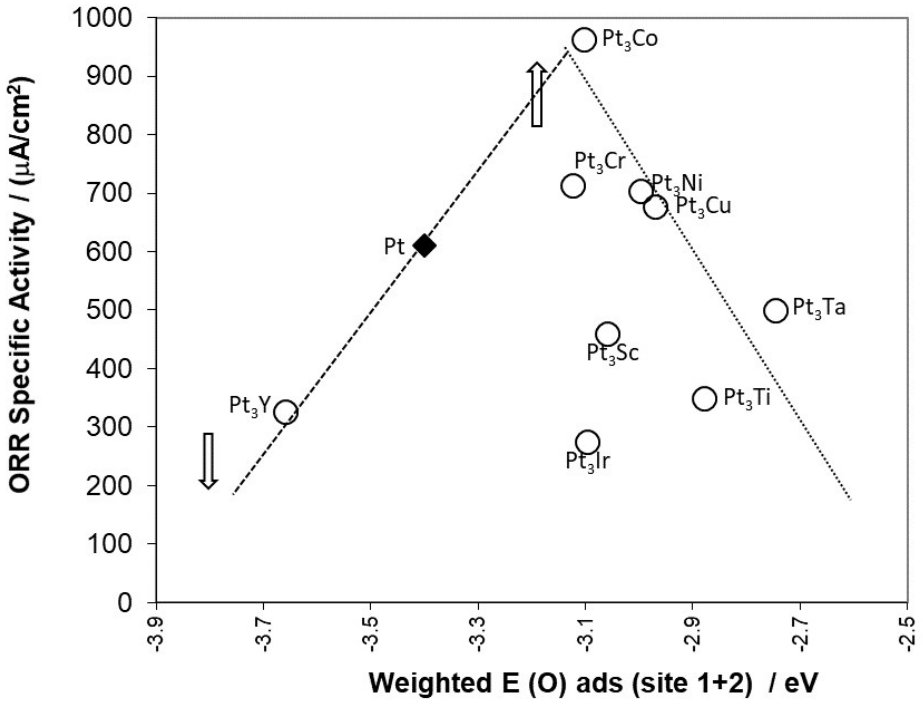

Figure 10. O_2 reduction specific activity at 900 mV as a function of weighted O_{ads} energy.

As there are a ratio of 3:1 O-Pt(Pt) sites to O-Pt(M) sites we have used a weighted binding energy to correlate to the O_2 reduction activity.

In contrast to the correlation of ORR activity with d-band centre, there appears to be a good 'vocano'-like relationship for the Pt-skin surfaces. The only exception to this is the Pt_3Ir system.

We have also investigated the correlation with a segregated surface.

Correlations with d band and O_{ads} of O segregated Pt_3M surfaces

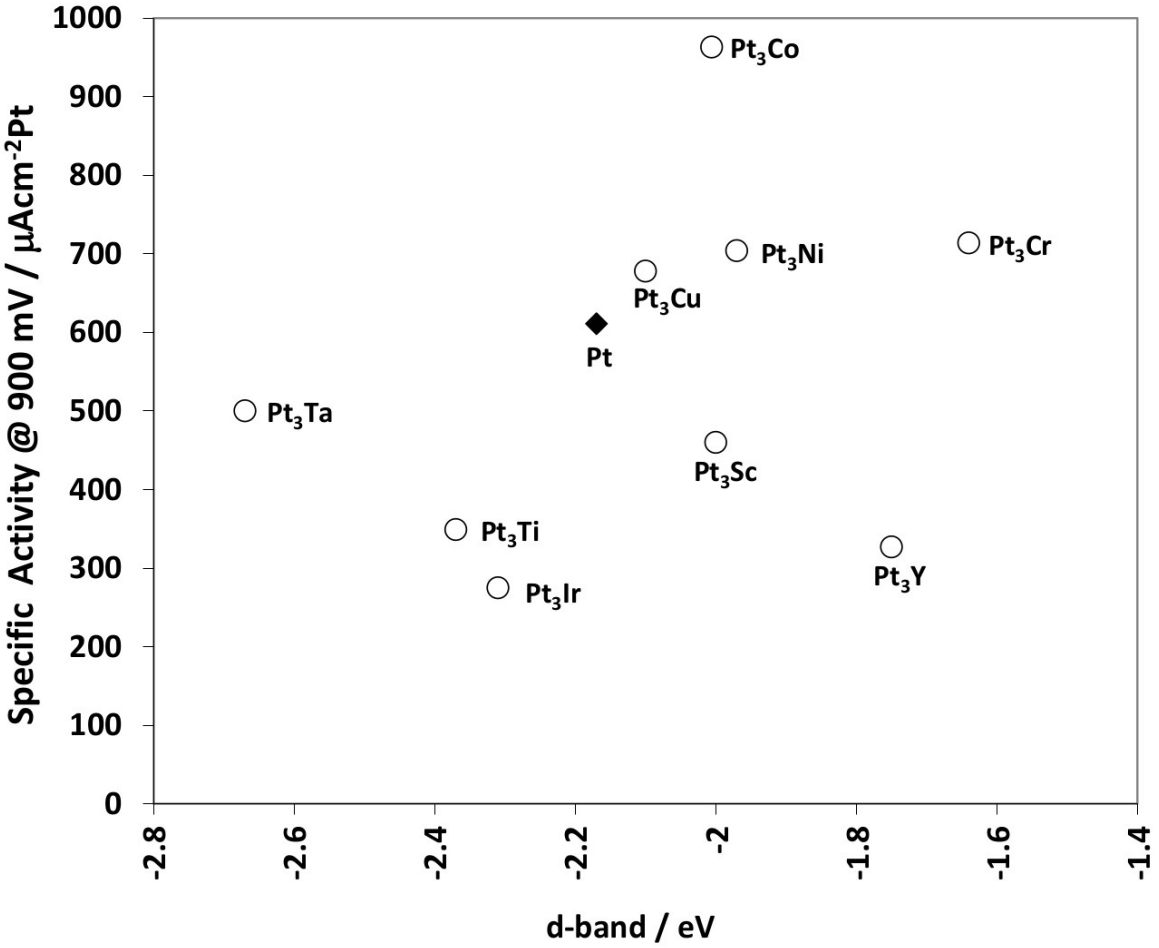

Figure 11a. O_2 reduction specific activity at 900 mV as a function of segregated surface d-band centre energy

There is a poor correlation between the segregated surface d-band centre and O_2 reduction activity,

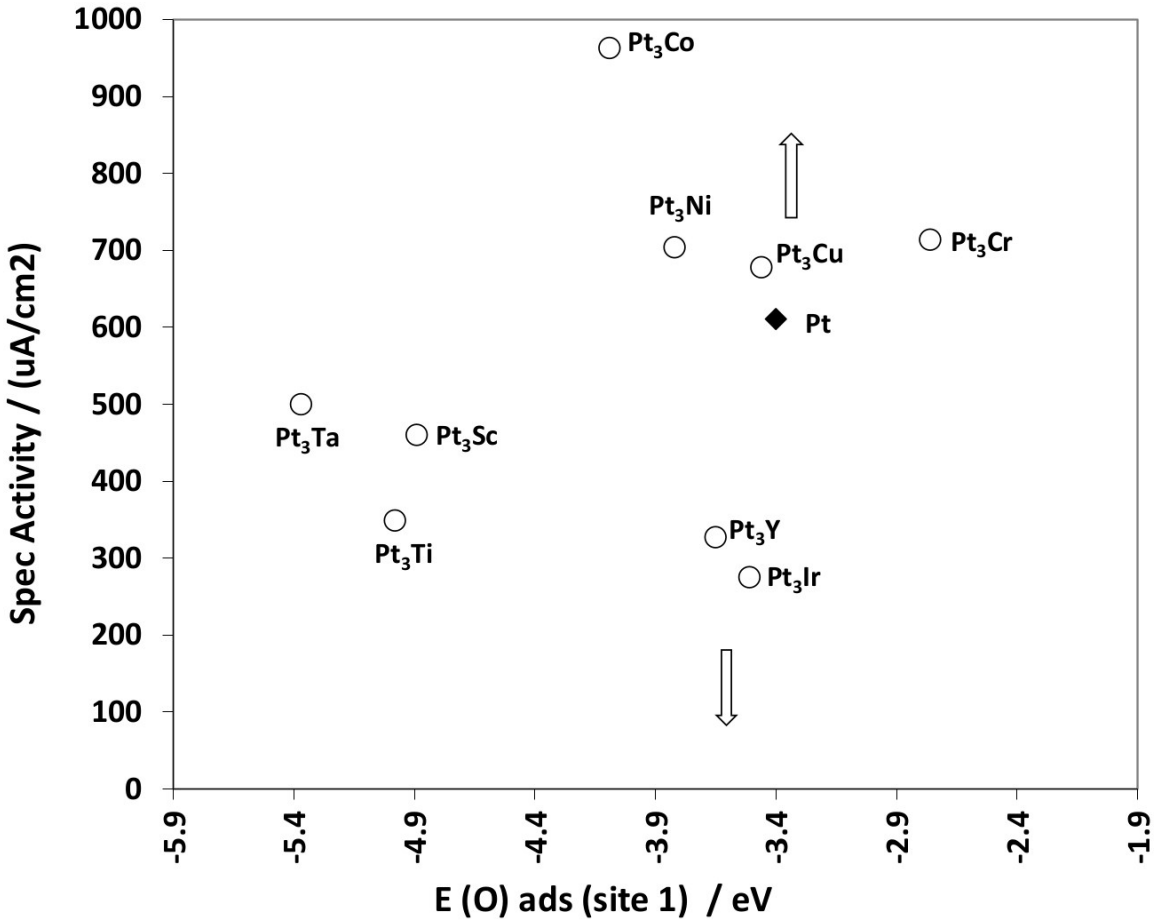

Figure 11b. O_2 reduction specific activity at 900 mV as a function of O induced segregated O_{ads} energies (site 1).

The binding energies of the segregated surfaces are generally much higher than that for the Pt skin surfaces (see Figure 7) and based on the correlation shown in Figure 6 would be expected to be poor surfaces for O_2 reduction. This suggests that under operating conditions, Pt_3M surfaces generally form Pt skin surfaces due to acid leaching of surface M.

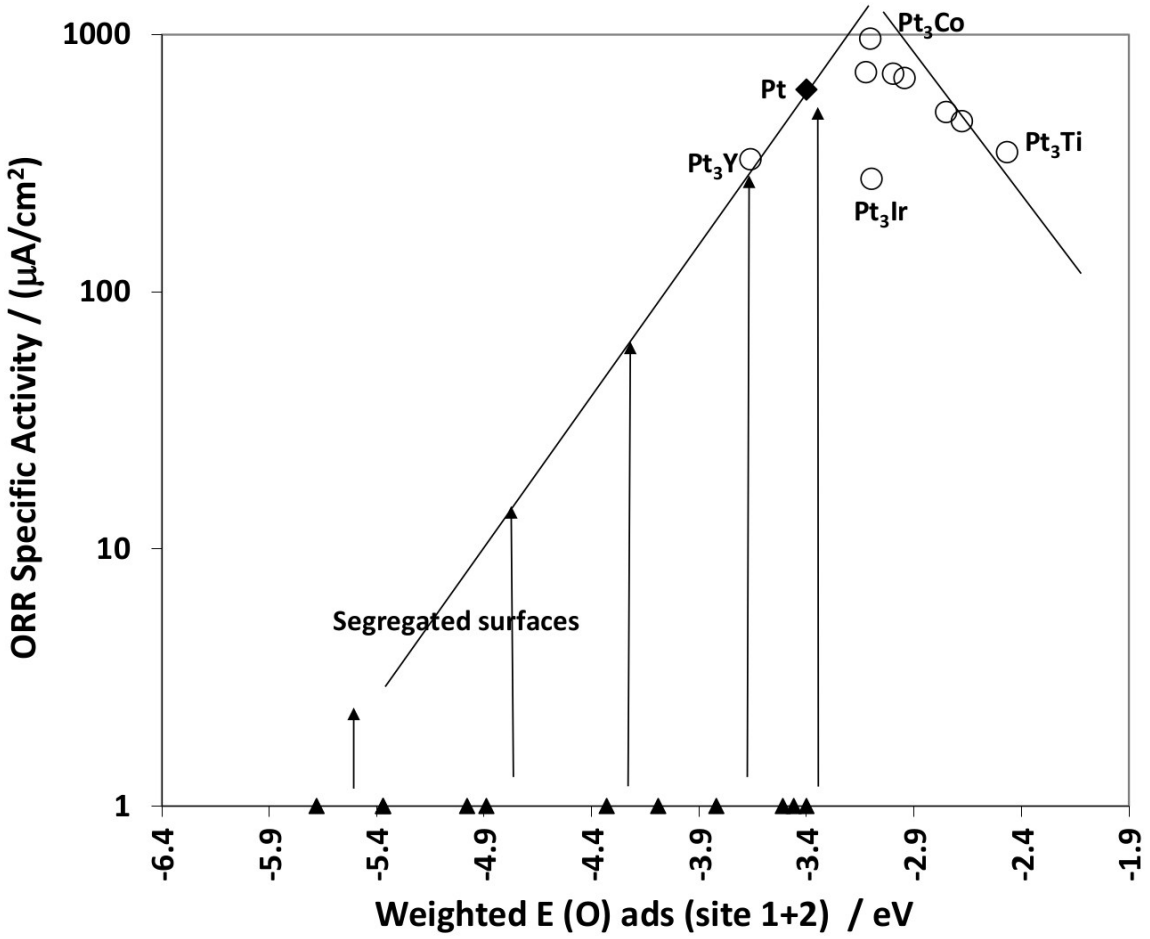

Figure S7. O_2 reduction specific activity as a function of a) weighted O_{ads} energy for Pt skin surfaces (○) and b) O_{ads} energy (site 1) for M segregated surfaces (□). The lines represent a rough volcano plot for the Pt skin data and the arrows represent possible mapping of the segregated surface data on to this volcano.

The comparison between the Oads for the Pt-skin surfaces and the O segregated surfaces are shown in Figure S7. The ORR activity is plotted as a log plot and volcano lines have been added for the Pt skin data. As all the segregated Pt_3M surfaces show O adsorption energies that are higher than Pt, it would be expected that ORR actvity will be lower than Pt, hence the mapping of the O_{ads} values to the left hand side of volcano.

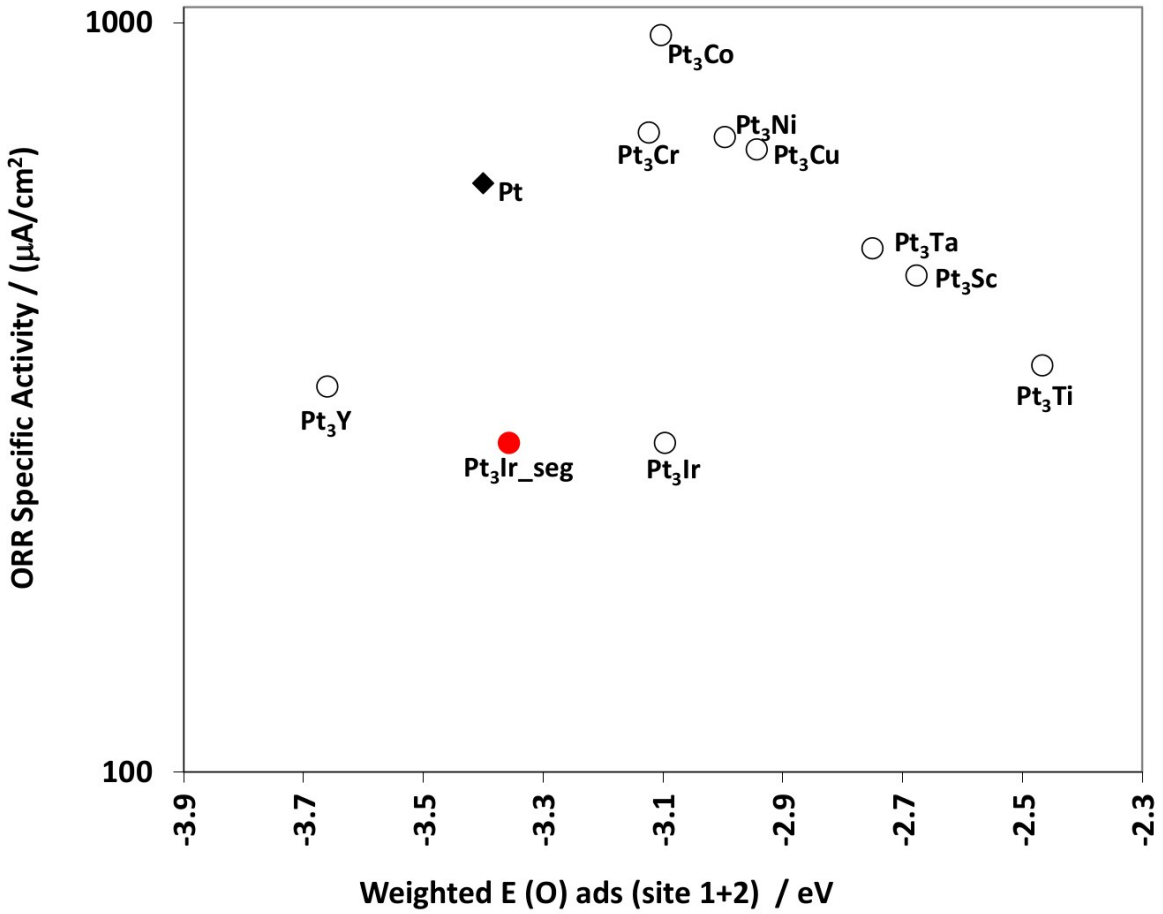

Figure S8. Figure 10 with Pt_3Ir O segregated O_{ads} energy added

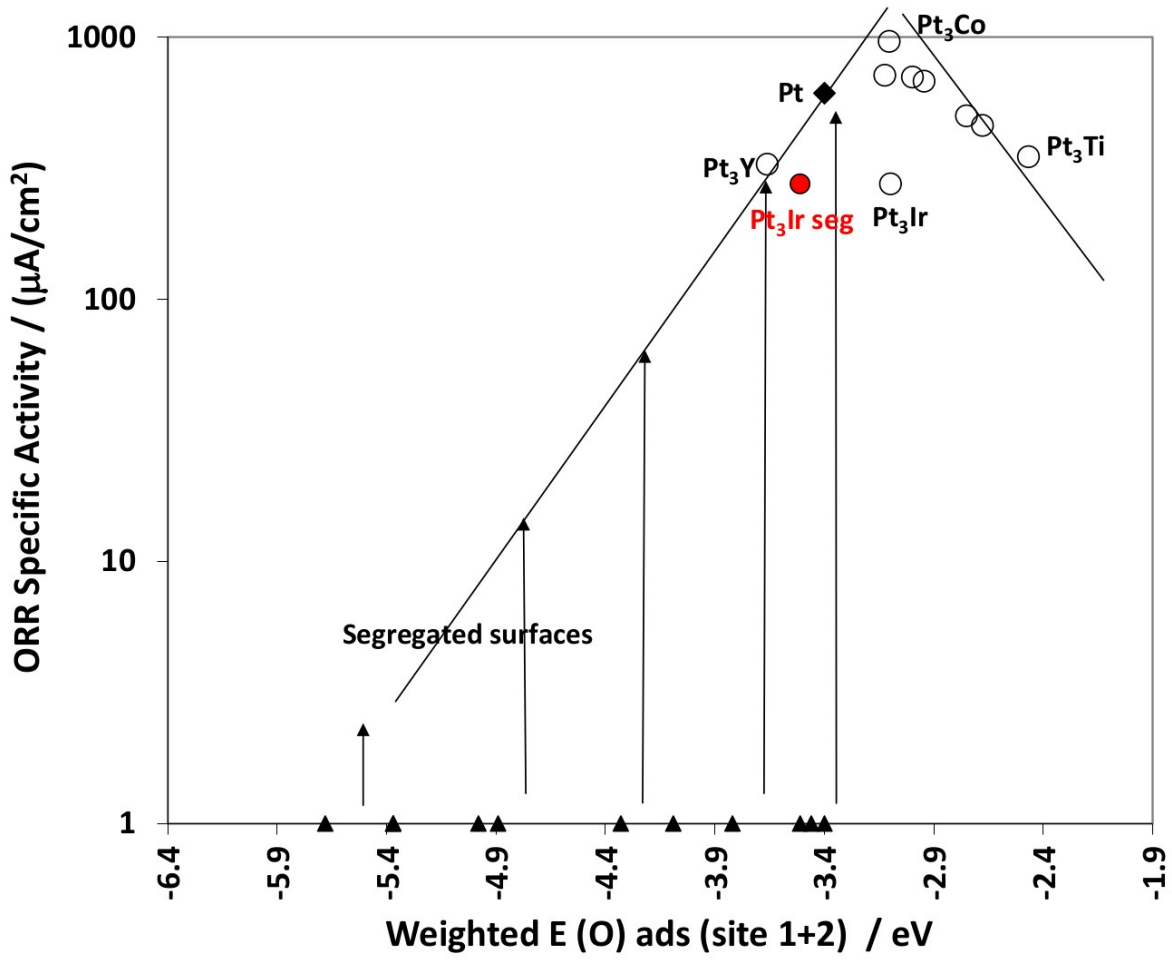

Figure S9. Figure S7 with Pt_3Ir O segregated O_{ads} energy value added

References

1. GB Patent 2242203, 'Catalyst Material comprising Platinum Alloy supported on carbon', J.S. Buchanan, G.A. Hards & S.J. Cooper, 25 Nov 1991
2. US Patent Application 2014/0205928, 'Ternary Platinum Alloy', S. Ball, T.R. Ralph, B.R. Theobald & D. Thompsett, 24 July 2014
3. S.C. Ball, R O'Malley, B.R.C. Theobald, E.L. Izzo, V.S. Murthi & L.V. Protsailo, J. Physical Chemistry C, 2013, 117, 23224
4. R.E. Benfield, J. Chem. Soc. Faraday Trans., (1992) 88, 1107